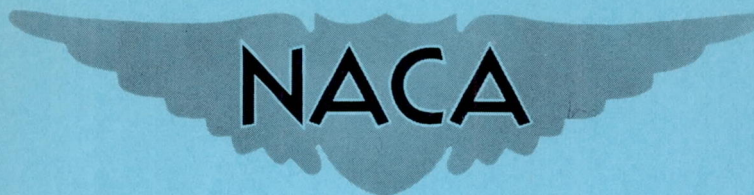


RM E52A09

NACA RM E52A09



RESEARCH MEMORANDUM

EXPERIMENTAL INVESTIGATION OF FLOW IN AN ANNULAR CASCADE
OF TURBINE NOZZLE BLADES OF CONSTANT DISCHARGE ANGLE

By Milton G. Kofskey, Harold E. Rohlik, and Daniel E. Monroe

Lewis Flight Propulsion Laboratory
Cleveland, Ohio

NATIONAL ADVISORY COMMITTEE
FOR AERONAUTICS

WASHINGTON
March 3, 1952

NATIONAL ADVISORY COMMITTEE FOR AERONAUTICS

RESEARCH MEMORANDUMEXPERIMENTAL INVESTIGATION OF FLOW IN AN ANNULAR CASCADE
OF TURBINE NOZZLE BLADES OF CONSTANT DISCHARGE ANGLE

By Milton G. Kofskey, Harold E. Rohlik, and

Daniel E. Monroe

SUMMARY

An investigation of the three-dimensional flow immediately downstream of an annular cascade of nozzle blades was made to obtain a good physical picture of the flow at blade-hub discharge Mach numbers of 1.18, 1.31, and 1.41. The blades were designed for axial entry and a constant discharge angle of $59^{\circ} 45'$ from axial.

The energy loss core at the blade tip was found to decrease in size with increasing Mach number and did not seem to affect appreciably the general pattern of angle distribution. The loss core at the blade hub, however, increased in size with increasing Mach number, and at the higher Mach numbers the center of the loss core was found to be in the region of large discharge angle gradients in the blade wake.

Losses near the hub showed a considerable increase with increasing Mach number, while losses near the tip showed a slight decrease. Overall mass-averaged blade efficiencies were found to be 0.983, 0.980, and 0.978 for hub Mach numbers of 1.18, 1.31, and 1.41, respectively.

The trend in angle variation across a flow passage was toward a lower discharge flow angle along the pressure side of the wake as Mach number was increased. This was true particularly near the high-loss region at the hub, where steep local angle gradients were obtained at the highest Mach number run.

INTRODUCTION

The design of turbine blades has largely been limited to the application of modified two-dimensional flow theory. The complex internal aerodynamics actually encountered in a turbine, however, have not been extensively investigated because satisfactory performance has generally been obtained through the use of the two-dimensional design methods, although these methods do not account for a large percentage of the

losses obtained in actual turbine operation. As gas velocities through turbines are increased to obtain the increased power and mass flow, the effects of radial gradients in pressure, velocity, and circulation at transonic conditions become increasingly important. If increases in efficiency, work per stage, and mass flow per unit frontal area are to be realized, an understanding of the problems introduced by three-dimensional flow must be obtained.

In order to obtain a better understanding of the effects of radial gradients in the flow, an investigation is being made of the flow immediately downstream of an annular cascade of turbine nozzle blades with such flow conditions. Detailed data on the three-dimensional flow immediately downstream of a set of nozzles have been obtained at the NACA Lewis laboratory at circumferentially averaged hub discharge Mach numbers of 1.18, 1.31, and 1.41. Particular emphasis was placed on the nature of the cores of high energy losses occurring along the inner and outer shrouds.

The purpose of this report is to present a preliminary analysis of the nozzle total-pressure loss and discharge flow angle as they exist under conditions of exit angle of $59^{\circ} 45'$ and Mach numbers as high as 1.4.

APPARATUS

Test unit. - A schematic view of the test unit used in this investigation is shown in figure 1. A filter was installed in a large depression tank (not shown in fig. 1) upstream of the test section to prevent damage and clogging of the delicate instruments by dirt particles from the air supply. The filter consisted of two layers of filter paper separated by two layers of 1/4-inch felt with both supported by wire mesh screening. A second depression tank downstream of the first tank (fig. 1) is located approximately 6 blade-tip diameters upstream of the nozzle blades. A long-radius calibrated nozzle was installed in the depression tank to measure the weight flow and to provide smooth entry into the duct leading to the nozzle blades in the test section. A fine mesh screen was also installed in the tank to give a uniform inlet velocity distribution. The air discharged from the nozzle blades into an annular duct having six straightening vanes located approximately 3 tip diameters downstream of the nozzle blades. The straightening vanes served to turn the flow to the axial direction and thus eliminated the possibility of reverse flow at the hub back toward the nozzle blades.

The camber of the straightening vanes was considerably modified to investigate whether the straightening vanes had any effect on the discharge flow from the nozzle blades. Surveys at the nozzle discharge indicated that the flow was insensitive to large changes in the straightening vane configuration.

Nozzle blades. - The nozzle blades used in the investigation were designed for a constant discharge angle of $59^{\circ} 45'$ from axial and for an equivalent weight flow of approximately 15.3 pounds of air per second.

The 48 blades of the turbine nozzle cascade (figs. 2 and 3) have a hub-to-tip radius ratio of 0.730, with a tip diameter of 16.25 inches. The blades have a solidity of 1.505 at the hub and 1.484 at the tip. The blade chord and trailing-edge thickness vary from respective values of 1.579 and 0.040 inch at the tip to 1.170 and 0.026 inch at the hub.

INSTRUMENTATION

The cascade was instrumented to determine the total and static pressures at the inlet measuring station located 0.5 inch upstream of the tip section of the blades (fig. 3) and total pressures, wall static pressures, and flow angles at the discharge measuring station (fig. 3) located 0.159 inch downstream of the trailing edge of the nozzle blade tip. The instruments used to obtain the detailed surveys of the gas state at the inlet and discharge are shown in figure 4.

Total-pressure measurements. - Two types of total-pressure probe were used to measure total pressure in the blade passage; one type was designed specifically for measurements in the boundary layer, whereas the other probe was designed for free-stream measurements.

The pressure measuring head of the boundary-layer probe (fig. 4(a)) consists of 0.015-inch outside diameter tubing. The tip was flattened to approximately 0.003-inch inside minor axis length to obtain closer approximations of point values in the regions of high radial pressure gradients.

The three-dimensional total-pressure probe (fig. 4(b)) was designed to measure the total pressure outside the boundary layer for radial flow angles within the limits of approximately $\pm 12^{\circ}$. The probe consists of five 0.015-inch outside diameter tubes projecting 0.120 inch from the probe axis. The tubes are set at angles of 3° , 6° , -3° , -6° , and 0° from a plane normal to the axis of the probe and with the measuring ends of the tubes in this plane.

A shielded total-pressure probe was used to measure the reference total pressure at the inlet to the blades.

Static-pressure measurements. - Wall static taps of 0.015-inch diameter are located at both the hub and tip in the inlet and discharge measuring planes. At the inlet measuring plane, one static tap each at the hub and tip is located at the circumferential position used for inlet radial surveys.

Angle measurements. - A double-wire hot-wire anemometer probe (fig. 4(c)) was used to measure the discharge flow angles. The instrument consists of a pair of vertical parallel wires, supported by two prongs and mounted under tension. The center line between the two wires lies on the axis of the probe. Each of the wires has a diameter of 0.0009 inch and a length of approximately 0.045 inch. The distance between wire centers is 0.005 inch. The prongs are Inconel; the wires are 80 percent platinum and 20 percent iridium. Details of the prongs and the general construction of the hot-wire probes is discussed in reference 1. The application of hot-wire anemometer probes for the measurement of discharge flow angles at the hub Mach numbers reported in this investigation is discussed in the appendix.

Repeatability. - Discharge total pressures in the free-stream, wakes, and boundary layers could be repeated within ± 0.05 inch of mercury during any time interval. Although the total pressure was found to fluctuate to a greater extent in the wakes and boundary layer than in the free stream, the reproducibility of ± 0.05 inch was maintained by observing the data when the reference static pressure was at the desired set value. Wall static pressures could also be repeated within ± 0.05 inch of mercury over any extended time interval. The flow angles at all three hub Mach numbers could be repeated within $\pm 0.5^\circ$.

PROCEDURE

Surveys of total and static pressures were made at the inlet measuring station and surveys of total pressures and flow angles were made at the discharge measuring station (fig. 3). Surveys were taken at each of three hub discharge Mach numbers of 1.18, 1.31, and 1.41. The reference inlet total pressure was held constant at 26.38 inches of mercury absolute and the inlet total temperature was maintained at 553° R for all surveys.

Inlet surveys. - Radial surveys of total pressure and static pressure were made at only one circumferential location at the inlet, since preliminary surveys indicated little measurable circumferential variation in either total or static pressures. One static tap each on the hub and tip furnished the static-pressure values for the end points. Preliminary angle surveys indicated little variation from the axial direction over the blade passage and the inlet velocity distribution was therefore satisfactory for the investigation.

Discharge surveys. - At the discharge measuring station, radial surveys of free-stream total pressure and angle were made in radial increments of 0.2 inch at seven circumferential positions spaced to cover a complete blade passage (fig. 5). Radial survey points, using the boundary-layer probe, were taken 0.004 inch apart where high gradients

of total pressure existed in the boundary layer. The accurate location of these severe gradients as well as the delicate structure of the boundary-layer probes required the scheme of using a low voltage electric circuit which indicated by a light when contact of the measuring probe with the hub was made. Because of the circumferential total-pressure gradients in the blade wake regions, circumferential surveys of total pressure were made to supplement the radial surveys (fig. 5). The spacing of the circumferential surveys was made according to the magnitude of the pressure gradients.

Free-stream total pressures were measured with the five-tube total-pressure probe (fig. 4(b)). Each of the five tubes was rotated into the main stream for maximum reading and the maximum total-pressure reading obtained from the readings of all five tubes was taken as the total-pressure value for the survey point.

Wall static-pressure values for the nozzle discharge were obtained from the static taps located in the discharge measuring plane at each of the seven circumferential positions relative to the blade passages corresponding to the circumferential positions used for the radial surveys. Static pressure was assumed to vary linearly from the hub to the tip at each circumferential position for purposes of velocity calculations.

As the static pressure was used for mass averaging and the passage was choked for all three pressure ratios, any small difference between the true static and assumed static pressures would have little effect on the mass flow.

RESULTS

The results are presented in terms of inlet pressure surveys and discharge surveys of pressure and turning angle. The effects of variation in turning angle on the turbine rotor angle of attack are also included.

Inlet pressure surveys. - The results of surveys taken at the inlet measuring station for the hub Mach number (adjacent to the boundary layer) of 1.41 are shown in figure 6. A constant total pressure was obtained over most of the flow passage and the measurable losses occurred at both the blade tip and hub because of the wall boundary layers. The combination of almost constant inlet total pressure, static pressure, and flow angle produced a velocity distribution which was considered satisfactory. Since the flow was choked for all three pressure ratios, results obtained for the other hub Mach numbers were similar and are therefore not included.

Discharge surveys. - At the measuring station, hub Mach numbers (adjacent to the boundary layer) were 1.18, 1.31, and 1.41 at the pressure ratios tested, and 0.86, 1.06, and 1.10, respectively, near the tip. Results of the total-pressure surveys and static-pressure-tap data are presented in figure 7 as contours of energy loss where this loss is defined as follows:

$$\text{Loss} = 1 - \eta = 1 - \frac{V_a^2}{V_i^2} = \frac{\left(\frac{P_2}{P_1}\right)^{\frac{\gamma-1}{\gamma}} - \left(\frac{p_2}{P_1}\right)^{\frac{\gamma-1}{\gamma}}}{1 - \left(\frac{P_2}{P_1}\right)^{\frac{\gamma-1}{\gamma}}}$$

where

η local blade efficiency, V_a^2/V_i^2

V_a actual velocity

V_i ideal velocity as determined by reference inlet total and local discharge static pressures

P_1 reference inlet total pressure

P_2 discharge total pressure

p_2 discharge static pressure

γ ratio of specific heats, taken as 1.40

The loss, then, depends on point values of static and total pressures at the exit of the blade row.

Total pressure was almost constant over most of the flow passage at the value of the reference inlet total pressure. Losses occurred in the end-wall boundary layers, blade wakes, and at the junctions thereof, where cores of loss were clearly defined at all pressure ratios tested. Losses in the blade wakes were small compared with those measured in the loss cores and shroud boundary layers.

Results of pressure surveys show a slight decrease in maximum loss in the core at the outer shroud with an increase in Mach number. This maximum loss was 0.34 at the lowest Mach number run, 0.32 at the intermediate run, and 0.28 at the highest Mach number run. In the inner shroud core the trend was reversed and the corresponding losses were 0.21, 0.41, and 0.67. Core loss areas showed similar trends. The net

over-all effect was an increase in mean loss with Mach number, with a shift of the major loss region from the outer to the inner portion of the passage. Changes in the loss picture with Mach number at any radial position are shown in figure 8, where circumferentially mass-averaged loss values are plotted against radius for the three Mach numbers tested.

Data taken in the investigation described in this report were also used to obtain blade efficiencies for the three Mach numbers tested. Mass averaged blade efficiencies for the three Mach numbers were 0.983, 0.980, and 0.978 in order of increasing Mach number. These values, however, are all slightly high by approximately 0.002 as the inlet velocity was neglected in the mass averaged efficiency equation. Although the mass averaged blade efficiencies are high and apparently satisfactory, they are not a good index of blade performance. The greatest accumulation of losses is at the junction of the blade and the hub, where velocities and velocity gradients are greatest, thereby making the flow highly unstable and inducing additional viscous losses and large angle gradients.

The velocity coefficients which are the square root of the blade efficiencies were 0.992, 0.990, and 0.989 in order of increasing Mach number.

Results of discharge angle surveys are shown in figure 9 as contours of discharge flow angle. Angle gradients shown here become larger with increasing Mach number, particularly near the hub. At a radial distance of 0.10 inch from the hub the variation in discharge angle across a passage increased from 2.4° to 8.5° to 25.0° as hub Mach number was increased from 1.18 to 1.31 to 1.41. These variations were serious only near the hub, however, and at the blade midspan the variation across a passage changed little with Mach number. At the two higher Mach number runs the gradients were most severe in the blade wake near the hub and in the corner of the passage bounded by the pressure side of the wake and the hub.

Effects of the angle variations were determined by calculating rotor blade angles of attack at three radial positions for the highest Mach number run, where angle variations were greatest. For these calculations, an equivalent wheel speed of 8650 revolutions per minute was assumed. Discharge flow angle variations of 25.0° , 5.2° , and 5.3° at radial positions of 0.10 inch, 1.10 inches, and 2.10 inches, respectively, led to local variations in rotor blade angle of attack of 31.0° , 7.2° , and 7.2° . Variations in flow angle, then, may result in additional losses in the rotor because of the variation in angle of attack.

Weight flow. - Observed weight flow varied less than 1 percent with Mach number in the range investigated. Values used for comparison were averages of several measurements made at each Mach number. These measurements were made at intervals as pressure and angle surveys were being made.

DISCUSSION

Secondary Flow

Viscous losses occurring in the blade row appear at the measuring plane as loss cores and shroud boundary layers of varying thickness. The losses assume this distribution because of secondary flows induced in the passages by circumferential and radial gradients in pressure.

In references 2 and 3, discussions of secondary flows in cascades of airfoils are presented in detail. Briefly, the nature of the flows discussed is as follows:

In a curved channel there must be a pressure gradient to balance the centrifugal force on particles of a fluid moving through the channel. This pressure gradient exists in a cascade where the surfaces of two adjacent blades define a curved channel. In the channel-end-wall boundary layers the fluid has a lower velocity and requires a smaller pressure gradient to balance the centrifugal force. Consequently, since the free-stream pressure gradient exists almost unchanged in the boundary layers, a deflection of the flow toward the suction side of the passage is induced, as shown in figure 10 (with viscosity reducing circulatory flow back to pressure side).

As a result of this motion, the end-wall boundary layers become thinner at the pressure surface and thicker at the suction surface where a tendency toward the formation of cores of low momentum fluid occurs and where a tendency for flow separation is greatest. The secondary flows in the boundary layers also result in slight underturning near the boundary-layer interface and overturning of the air across the boundary layer as the end walls are approached.

The radial pressure gradient induces similar secondary flow in the blade boundary layers and wakes of the blades investigated, resulting in a slight radial flow toward the hub. This flow appears to be of lesser magnitude than that in the shroud boundary layers and results in a thinning of the blade wake near the tip.

Total-pressure surveys made in this investigation show the shroud boundary layers to be thinnest on the pressure side of the wake and thicker toward the suction surface, with cores of low momentum fluid on the suction side of the blade ends.

Angle measurements were not made within 0.10 inch of the walls because of the dimensions of the hot-wire probe and the insensitivity of the wire in regions of large radial gradients in angle. The total-pressure probe used in the boundary layers, however, indicated a sharp increase in turning angle as it was moved through the boundary layers

toward the walls. This increase was observed while the probe was rotated to obtain a maximum pressure reading. The change with radius in angular position of the probe at the maximum pressure reading appeared to be about 20° at some circumferential positions.

The shape of the discharge boundary layers, the presence of the loss cores, and the increase in turning angle in the boundary layers substantiate previous observations of secondary flows as described in references 2 and 3.

Loss Trends

Figures 7 and 8 show a shift of the major loss region from the outer part of the passage to the inner with increasing Mach number. This shift was accompanied by an over-all increase in mean loss with Mach number, and an actual decrease in mean loss in the outer part of the passage. The great increase in loss near the hub could be expected because of the higher velocities there, where the likelihood of shocks and flow separation from the blade surfaces is much greater. Since the decrease in mean loss near the tip was the result of a slight decrease in total-pressure loss as well as the decrease in static pressure, an inward radial flow of low momentum fluid upstream of the measuring plane is indicated. Such a flow would take place in the blade boundary layers and wakes, where velocities are low and the radial pressure gradient is not balanced by the centrifugal force of high-tangential-velocity fluid.

Discharge Angle Distribution

In figure 11 the circumferential average of discharge flow angle is plotted against radius for each of the Mach numbers tested. At each of the Mach numbers, the average angle was constant over most of the passage with a decrease near the hub. This decrease near the hub became more pronounced as Mach number was increased. The accumulation of low velocity fluid near the hub effectively blocked the flow and induced high axial velocities in the immediate vicinity. This effect is discussed more fully in reference 4. The result was a great circumferential variation in angle with a net decrease from the rest of the passage.

The results of the surveys described indicate some of the gradients encountered by a turbine rotor operating behind a cascade of blades having a constant discharge angle in the Mach number range tested, and the effect of Mach number on blade efficiency. The dependence of angle and velocity gradients on the development of losses shows the need for controlling both the increase in loss with Mach number and the accumulation of low momentum fluid near the hub.

SUMMARY OF RESULTS

The following results were obtained in an investigation of an annular cascade of turbine nozzle blades designed for axial entry and a constant discharge angle of $59^{\circ} 45'$ and tested at hub Mach numbers of 1.18, 1.31, and 1.41:

1. Cores of energy loss were clearly defined at the junctions of blade wakes and end-wall boundary layers at all Mach numbers tested.

2. Over-all integrated blade efficiency decreased with increasing Mach number. Although high efficiencies of 0.983, 0.980, and 0.978 were obtained for the three increasing Mach numbers, they are not a good index of blade performance. High loss cores occurring along the suction side of the blade, where diffusion is greatest and the flow is highly unstable, may result in flow separation or shock losses.

3. In the inner half of the passages surveyed, losses increased with increasing Mach number, whereas in the outer half the losses decreased.

4. The range of angle variation across a passage outside the wall boundary layers increased with Mach number, particularly near the hub, with lowest angles occurring along the pressure side of the wake. At a radial distance of 0.10 inch from the hub, circumferential variations in angle were 2.4° , 8.5° , and 25.0° at hub Mach numbers of 1.18, 1.31, and 1.41, respectively. The largest gradients involved in these angle variations existed in the regions of high loss. In the central portion of the blade passages, changes in the variation with Mach number were small.

5. The presence of the loss cores, the shape of the boundary layers, and the angles observed in the end-wall boundary layers are evidences of the existence of secondary flows which have been previously observed in other investigations. The secondary flows not only increase the energy loss by introducing rotation but pile up low momentum air along the suction side of the blade which may result in either flow separation or shock losses or both with the introduction of any slight disturbance.

Lewis Flight Propulsion Laboratory
National Advisory Committee for Aeronautics
Cleveland, Ohio

APPENDIX

APPLICATION OF HOT-WIRE ANEMOMETER PROBE

The hot-wire probe for measuring flow angles consists of two platinum and iridium alloy wires mounted in spatial and electrical parallelism. The wires are supported with their lengths perpendicular to the air stream and are mounted parallel to the axis of the probe and rotation. The alinement of the wires with the air stream is detected electrically by observing the maximum in potential drop when the downstream wire temperature reaches a peak as a result of receiving heat by convection through the wake from the upstream wire.

The electrical equipment used for the discharge flow angle investigation with the hot-wire anemometer probe consisted essentially of a Wheatstone bridge, a direct current power supply with which the current could be easily adjusted over a continuous range, a voltage amplifier, and a voltmeter for indication of the bridge output voltage. A probe actuator with appropriate switching arrangement was used to control the angular orientation of the hot-wire array with the air flow. The circuit employed in obtaining angle data, as well as the theory and procedure, is discussed in reference 1.

A compromise among wire sensitivity, effects of radial angle gradients, and wire life determined the size of the wires used for the investigation. A satisfactory wire life in the filtered air supply limited the wire diameter to a minimum of 0.0009 inch. The wire operating temperature of approximately 250° C and wire spacing of 0.005 inch gave good sensitivity. The wire length was kept small (0.040 in.) to reduce the effects of radial angle gradients. The extremely small wire diameter as compared with wire length resulted in a large wire length to diameter ratio and helped to increase the angle sensitivity and to minimize the probe effects on the wire operation.

Wire damage from collision by dirt particles in the air supply either made the probe inoperative or changed the original wire orientation, thereby changing the reference angle calibration. Frequent checking of a previous data point was therefore essential to prevent data errors resulting from change in wire orientation due to wire damage.

When the pair of heated wires was alined with the air stream, visual notation of the reversals of the change of bridge output voltage was found necessary. Several reversals were usually made to obtain an accurate angle value. The variation in a set of readings was on the order of $\pm 0.5^\circ$ for most series.

The reproducibility of the averages varied both with Mach number and flow conditions in the vicinity of the survey point. In the free-stream portions of the passage, the average flow angles could be repeated within $\pm 0.5^\circ$ at the three hub Mach numbers investigated.

In the regions of high pressure loss, more difficulty was encountered in finding a definite voltage reversal, and a larger variation in the angle orientation of the wire array was obtained before any noticeable changes in voltage were noticed. This decrease in sensitivity was greater in the total-pressure loss core. The angle data presented in these regions therefore represent the midpoints of plateaus of uniform voltage drop across the wire instead of peak voltage. The plateaus are probably due to turbulence or different steady flow conditions over various portions of the wire. In the severe cases, the plateaus were as much as 40° wide indicating regions of high vorticity.

Some angle data were obtained for radial positions within 0.1 inch of the hub, but these data were not of the desired accuracy and the results were therefore not included herein. The vertical parallel pair of wires, as used for this investigation, is not suitable for boundary-layer measurements because large radial angle gradients exist and the wire length limits the minimum radial distance between the survey point and the hub to approximately 0.035 inch.

REFERENCES

1. Lowell, Herman H.: Design and Applications of Hot-Wire Anemometers for Steady-State Measurements at Transonic and Supersonic Airspeeds. NACA TN 2117, 1950.
2. Lieblein, Seymour, and Ackley, Richard H.: Secondary Flows in Annular Cascades and Effects on Flow in Inlet Guide Vanes. NACA RM E51G27, 1951.
3. Carter, A. D. S.: Three Dimensional Flow Theories for Axial Compressors and Turbines. Rep. No. R.37, British N.G.T.E., Sept. 1948.
4. Goldstein, Arthur W.: Analysis of Performance of a Jet Engine from Characteristics of Components. I - Aerodynamic and Matching Characteristics of Turbine Component Determined with Cold Air. NACA Rep. 878, 1947. (Formerly NACA TN 1459.)

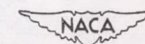
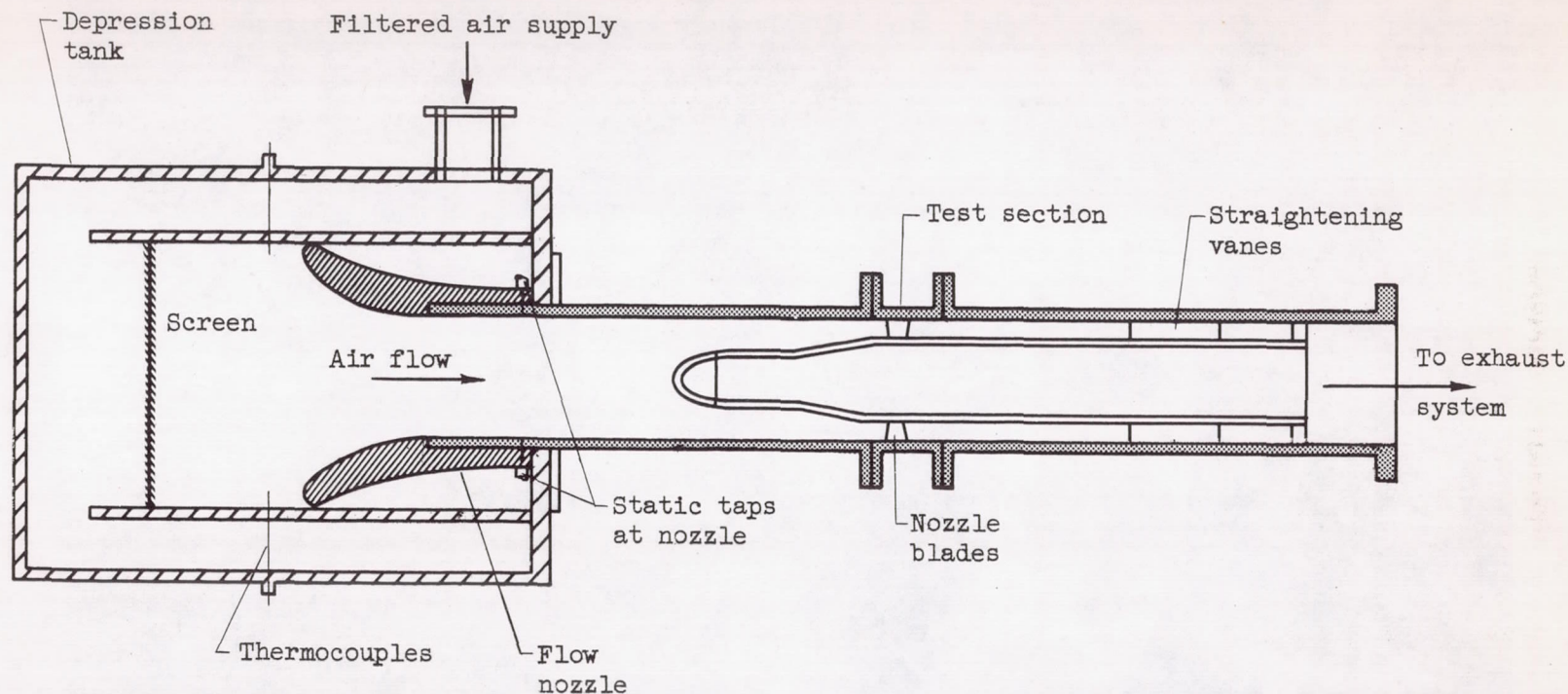


Figure 1. - Schematic view of annular nozzle cascade test unit.

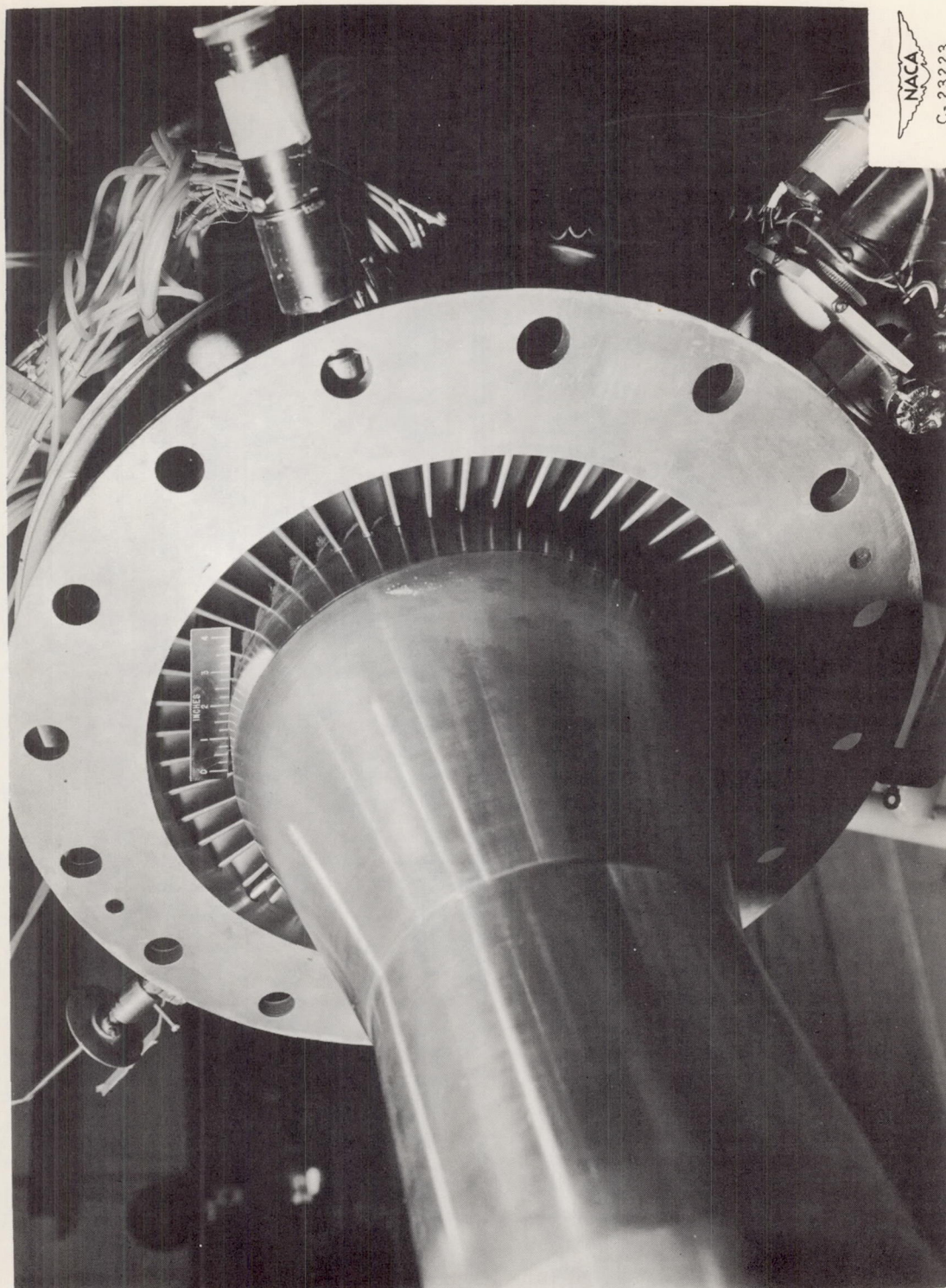
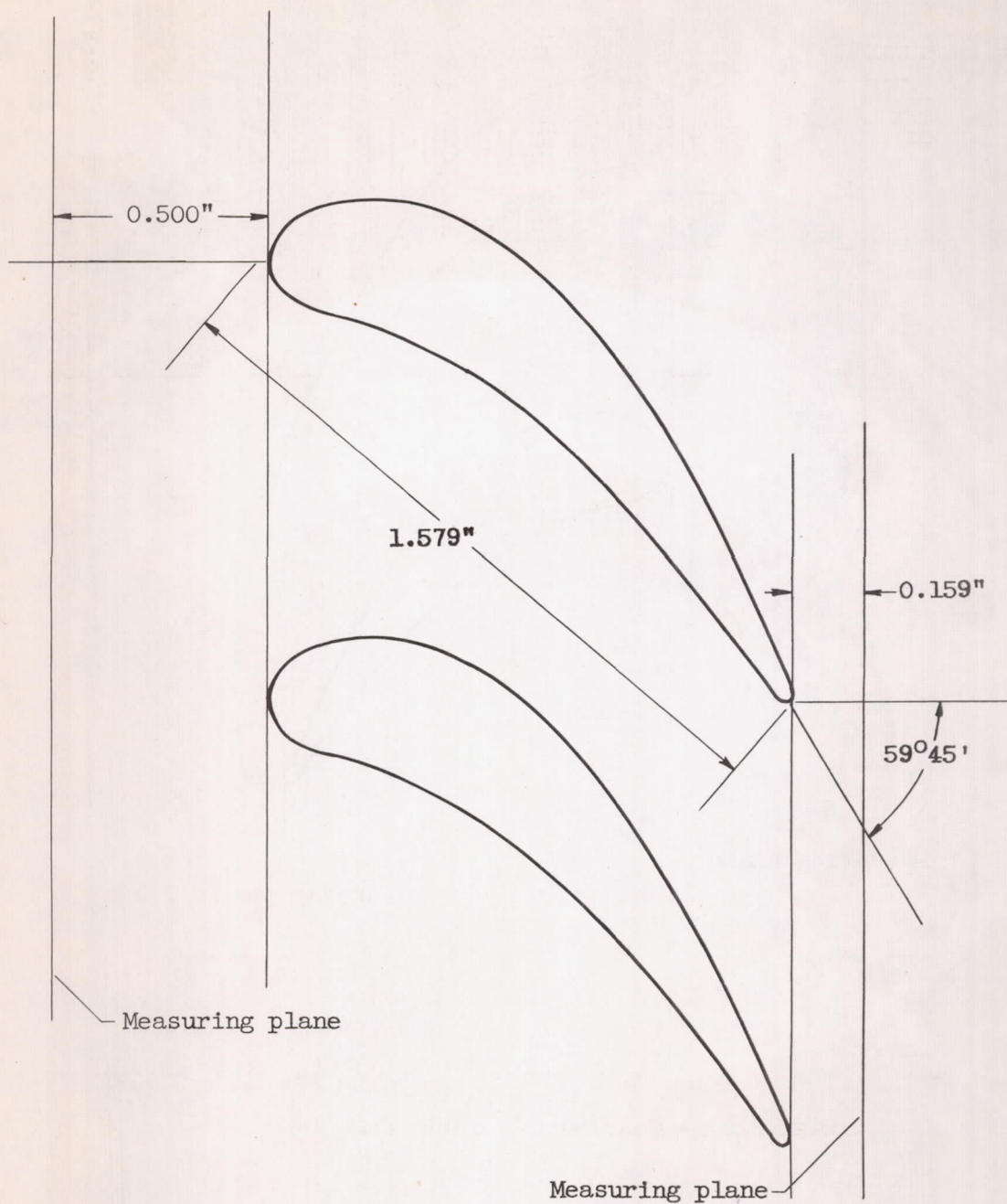
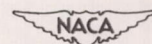


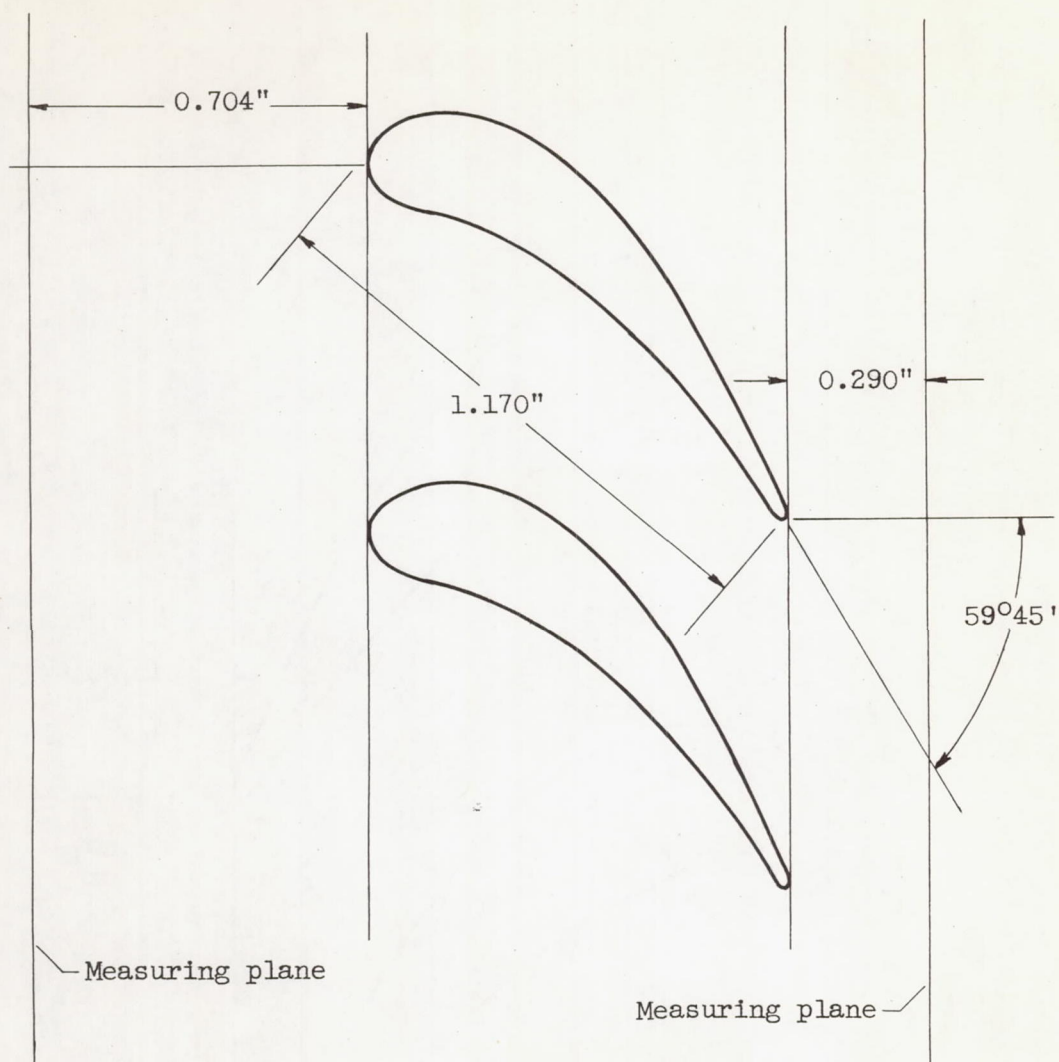
Figure 2. - Inlet of test section.



(a) Tip.

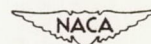
Figure 3. - Blade profile.

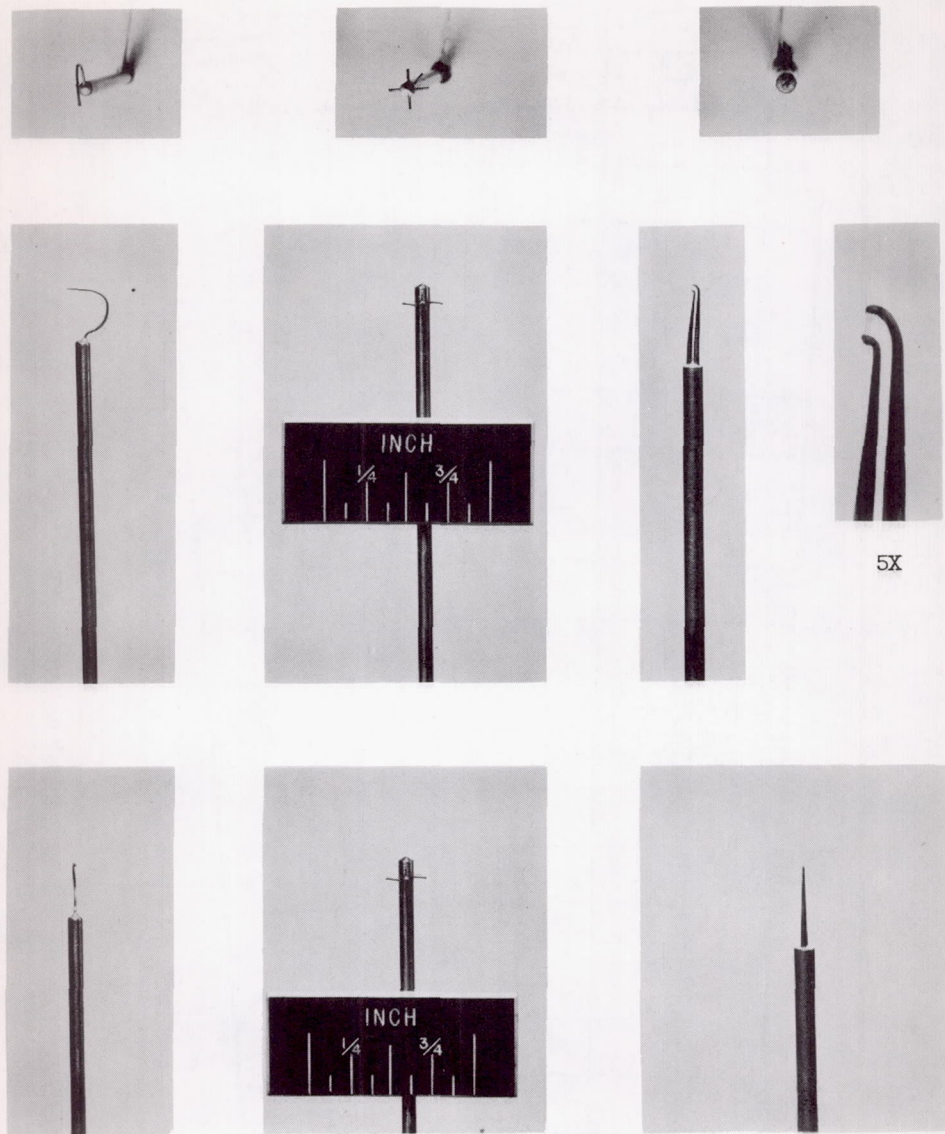




(b) Hub.

Figure 3. - Concluded. Blade profile.





(a) Boundary-layer probe. (b) Three-dimensional total-pressure probe. (c) Hot-wire probe.

Figure 4. - Survey instruments.

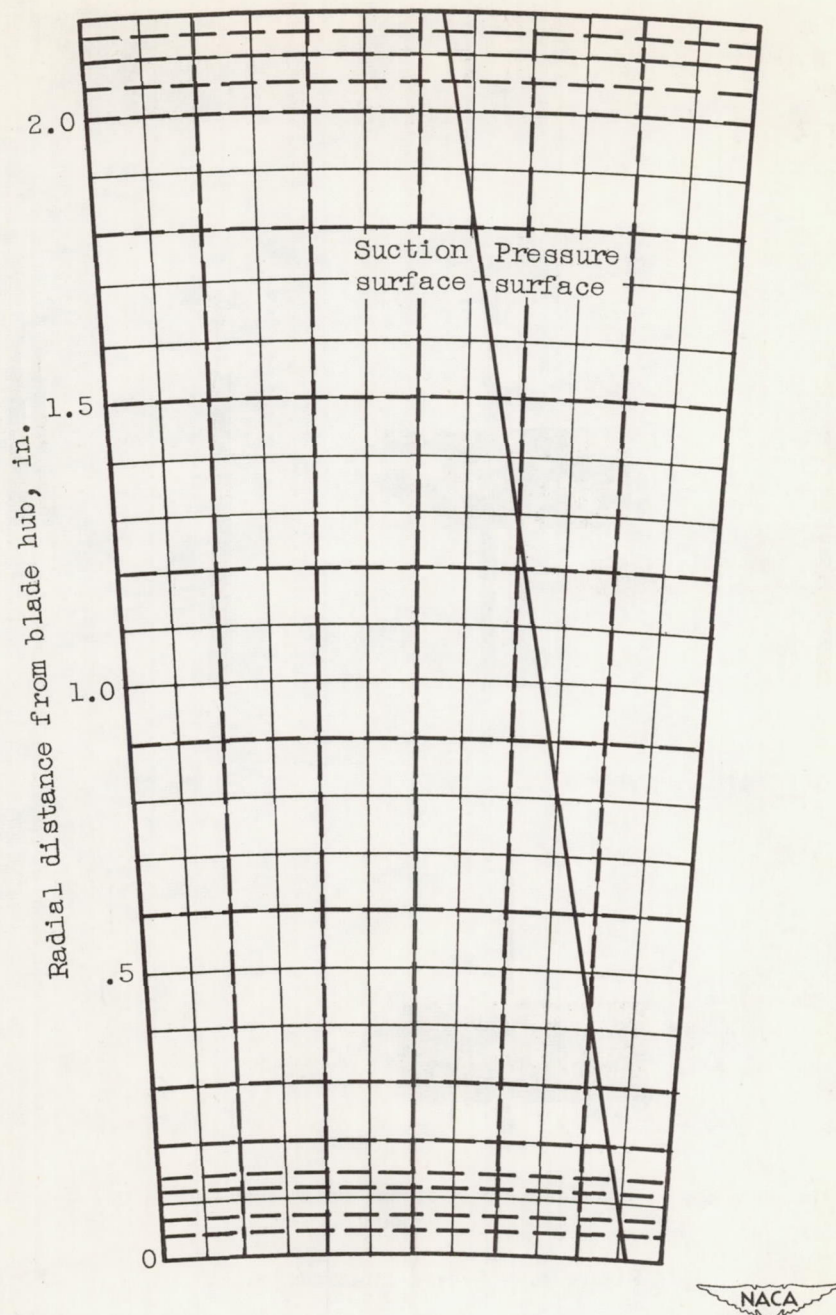


Figure 5. - Survey lines in discharge measuring plane and blade trailing-edge projection. (View looking downstream).

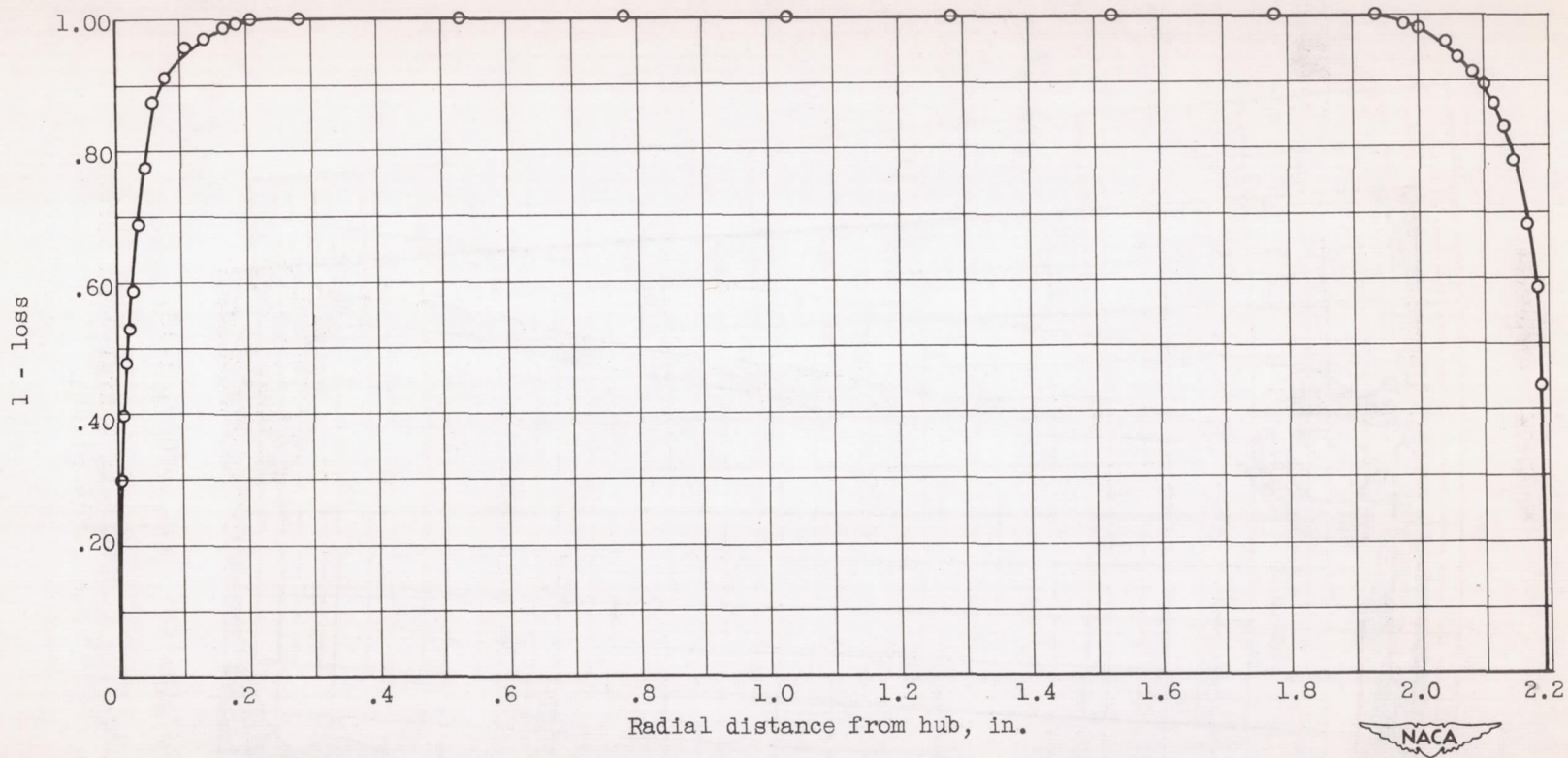


Figure 6. - Radial distribution of loss at inlet.

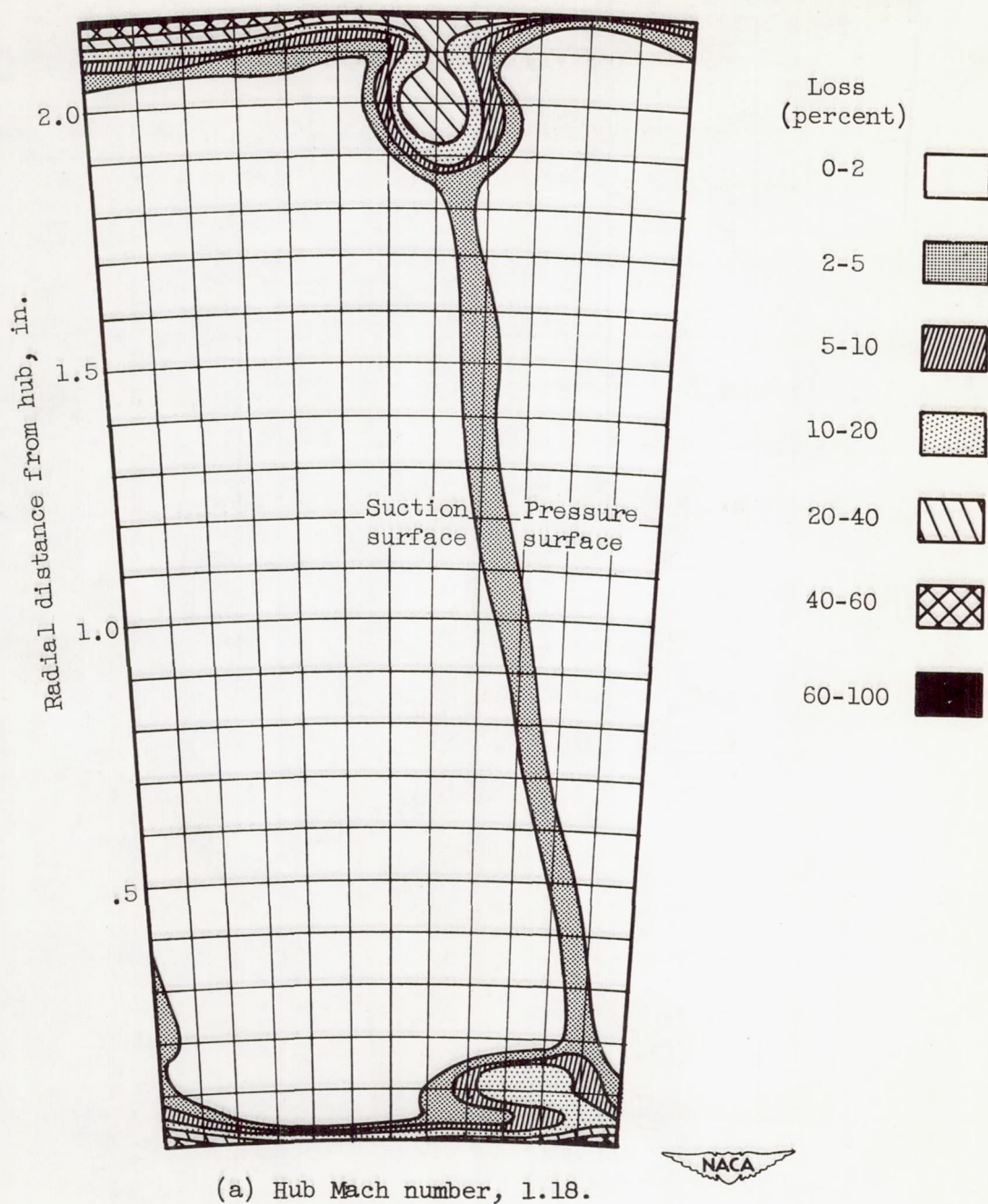
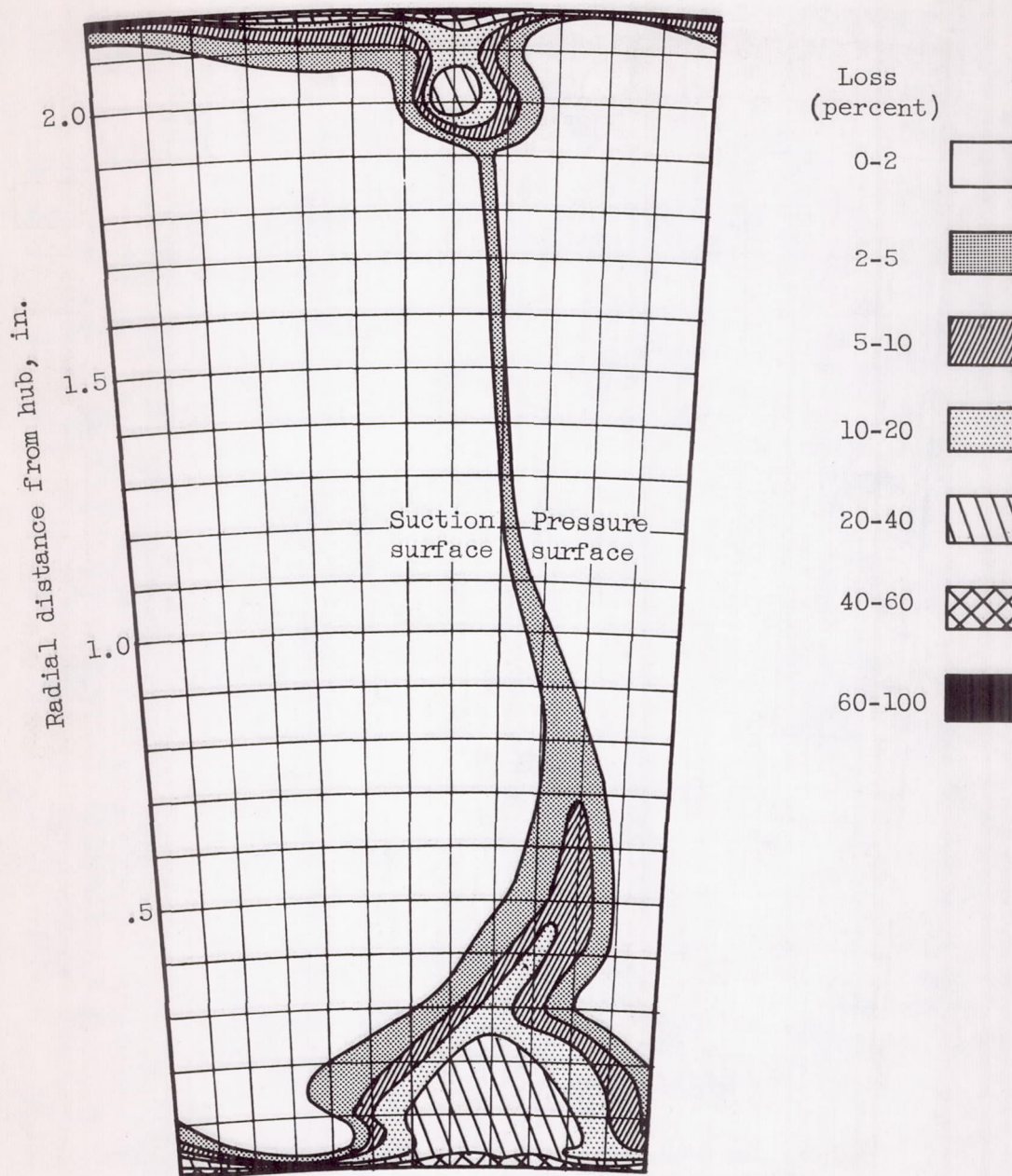
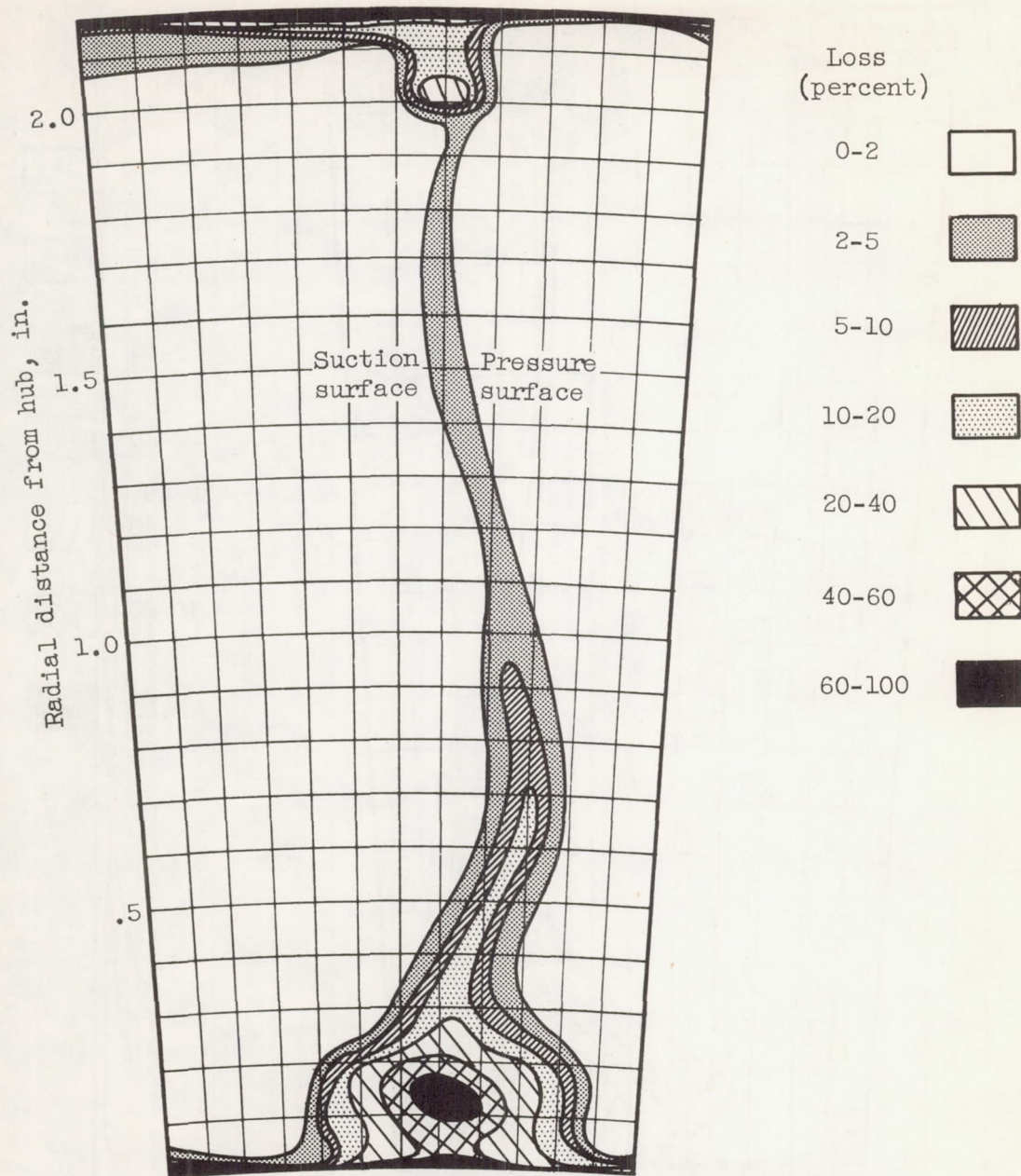


Figure 7. - Contours of energy loss across one blade pitch.



(b) Hub Mach number, 1.31.

Figure 7. - Continued. Contours of energy loss across one blade pitch.



(c) Hub Mach number, 1.41.



Figure 7. - Concluded. Contours of energy loss across one blade pitch.

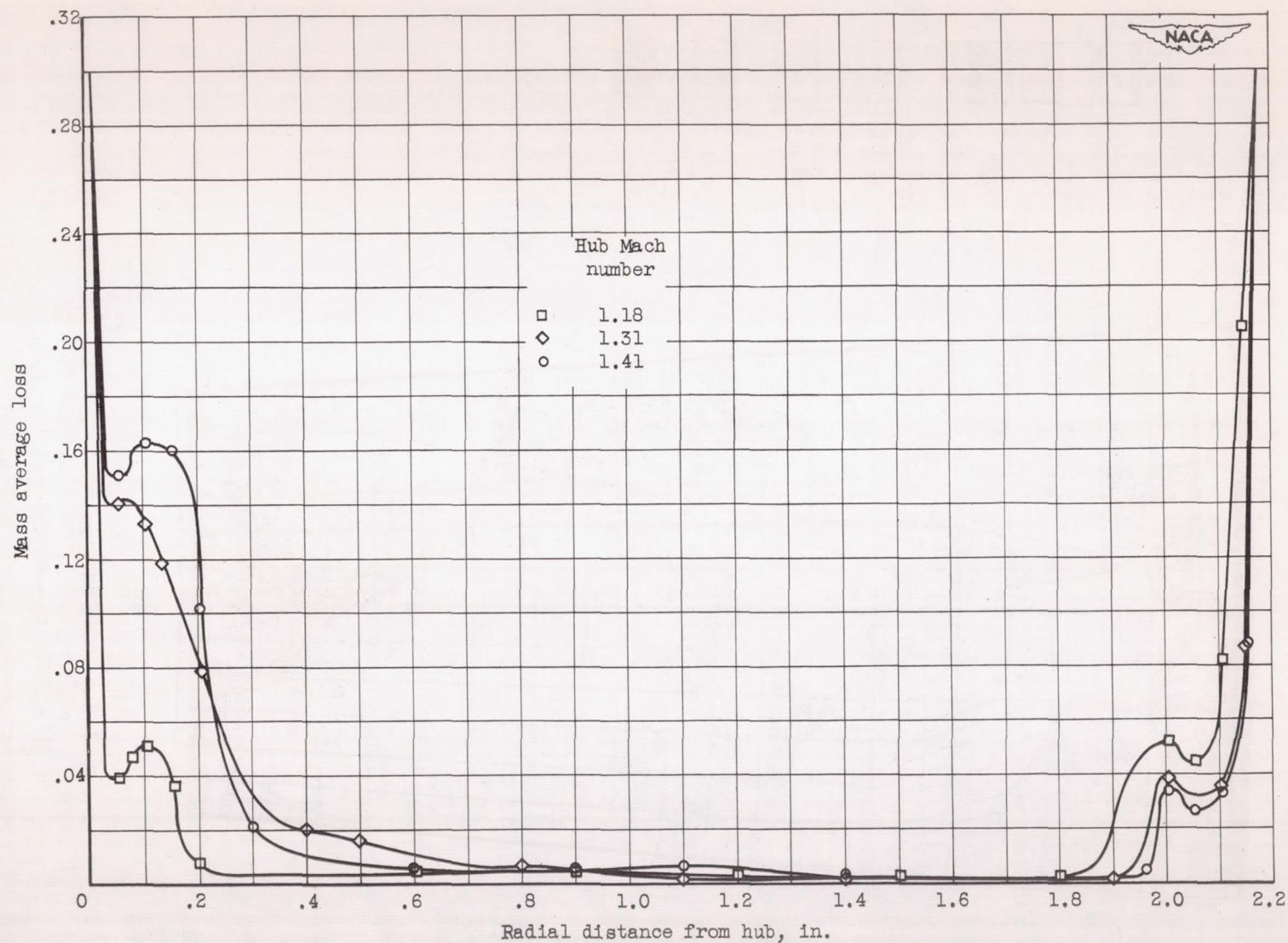
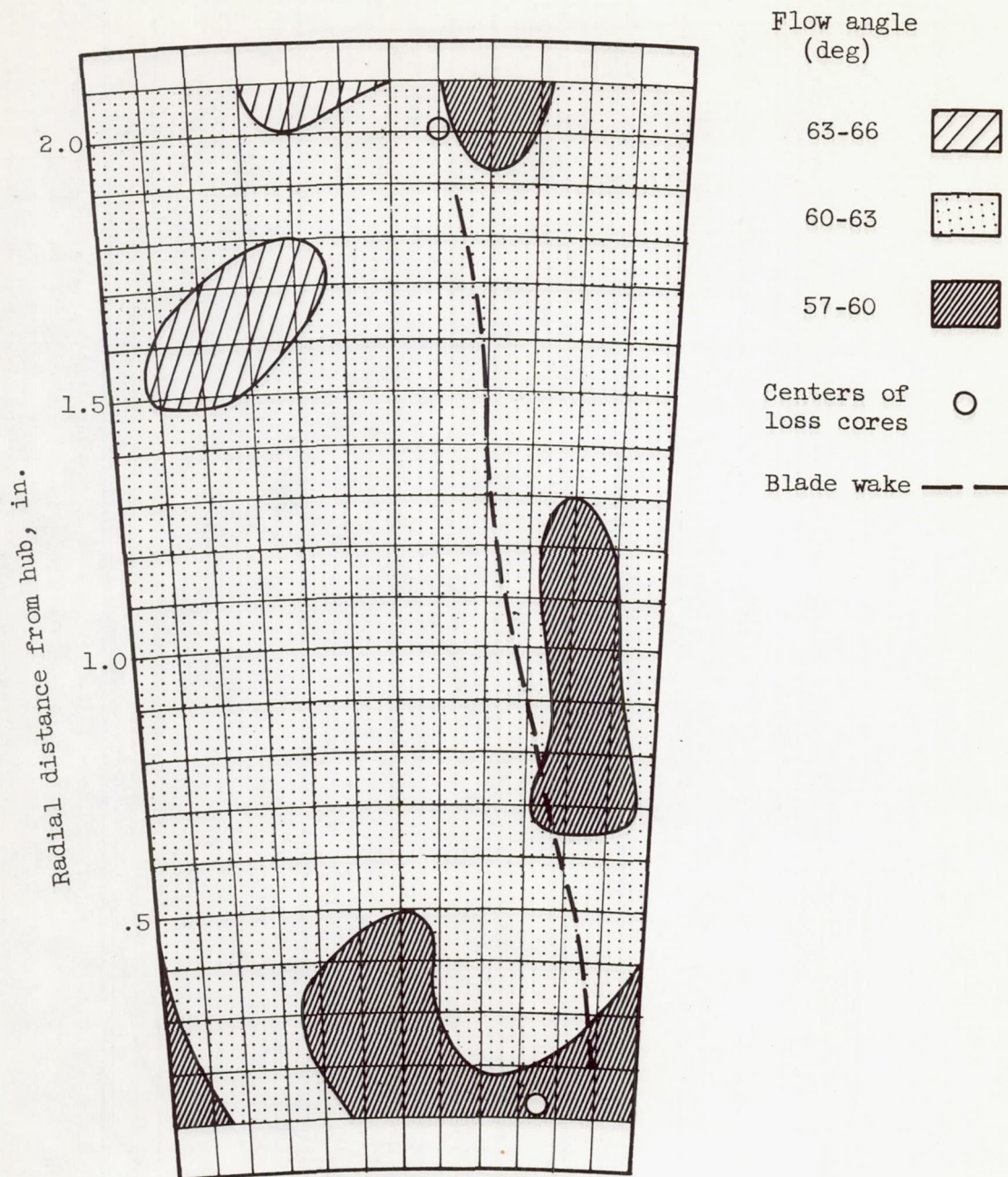


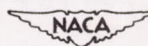
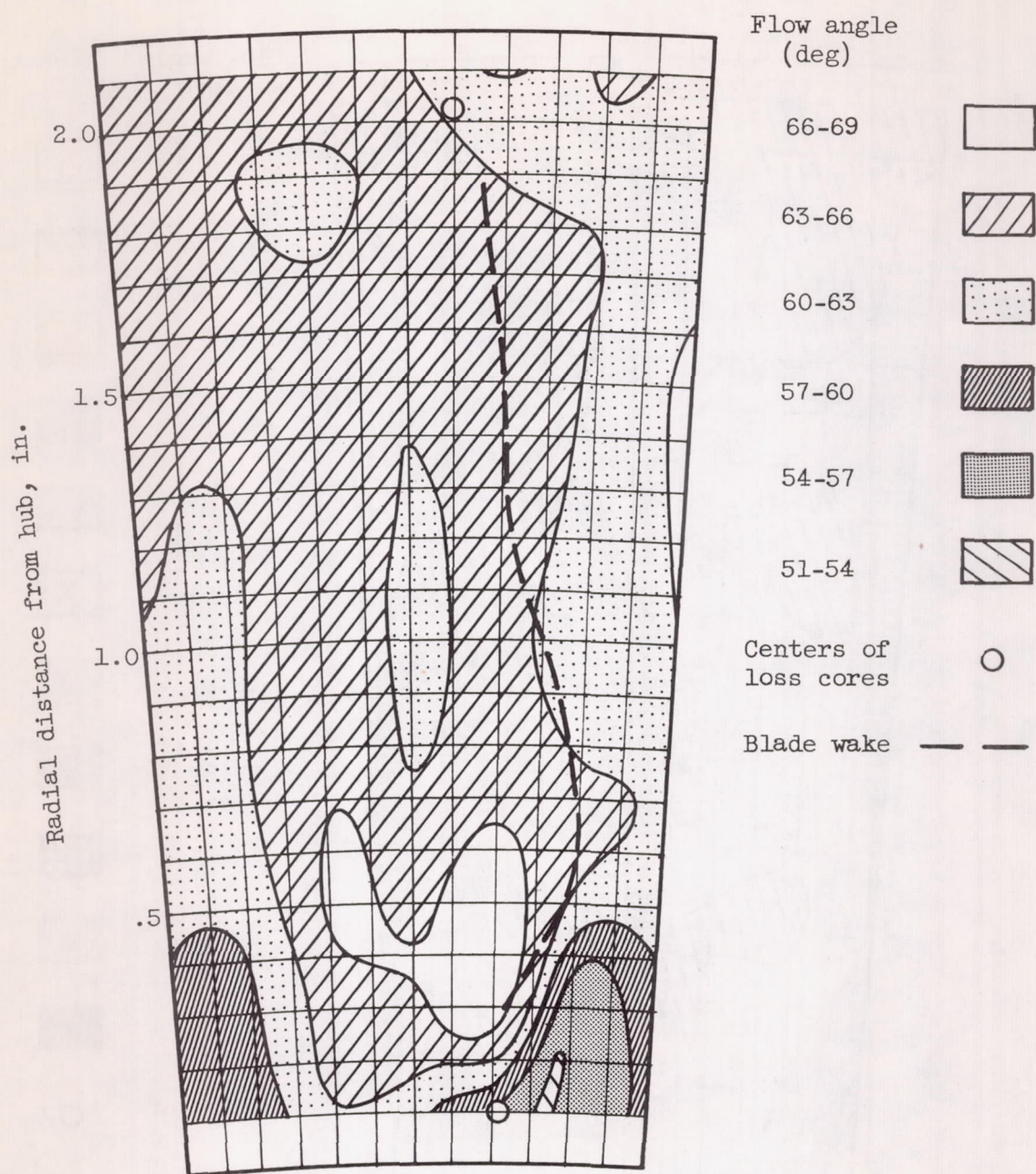
Figure 8. - Radial distribution of loss at discharge.



(a) Hub Mach number, 1.18.

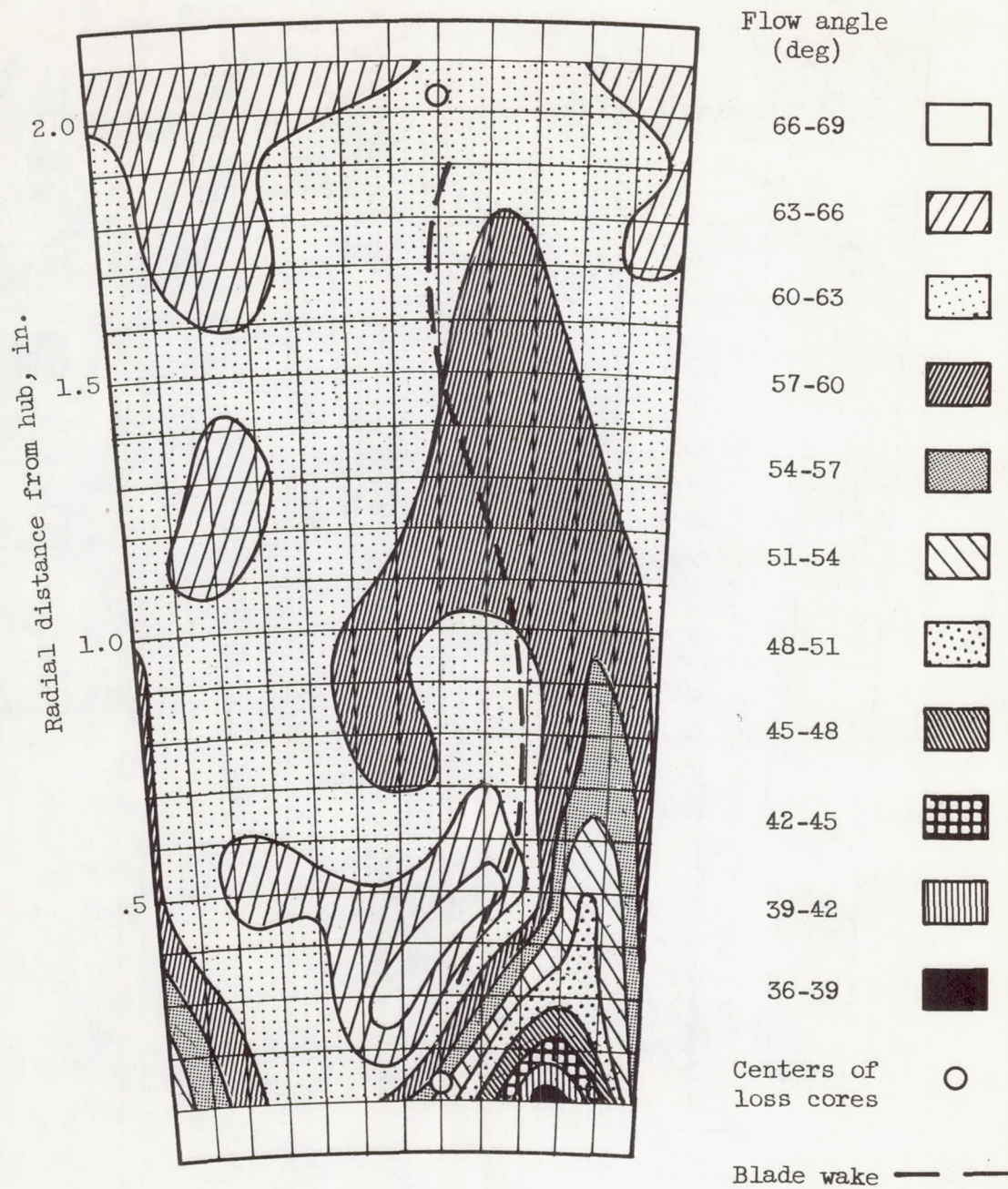


Figure 9. - Contours of discharge flow angle across one blade pitch.



(b) Hub Mach number, 1.31.

Figure 9. - Continued. Contours of discharge flow angle across one blade pitch.



(c) Hub Mach number, 1.41.



Figure 9. - Concluded. Contours of discharge flow angle across one blade pitch.

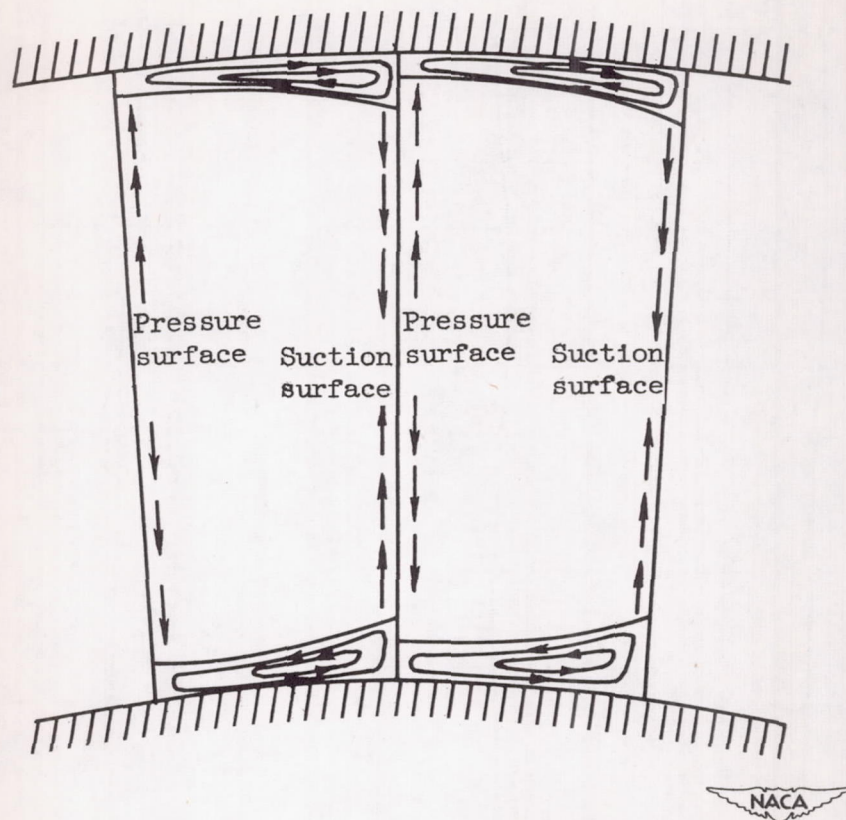


Figure 10. - Secondary flow components in two blade passages.

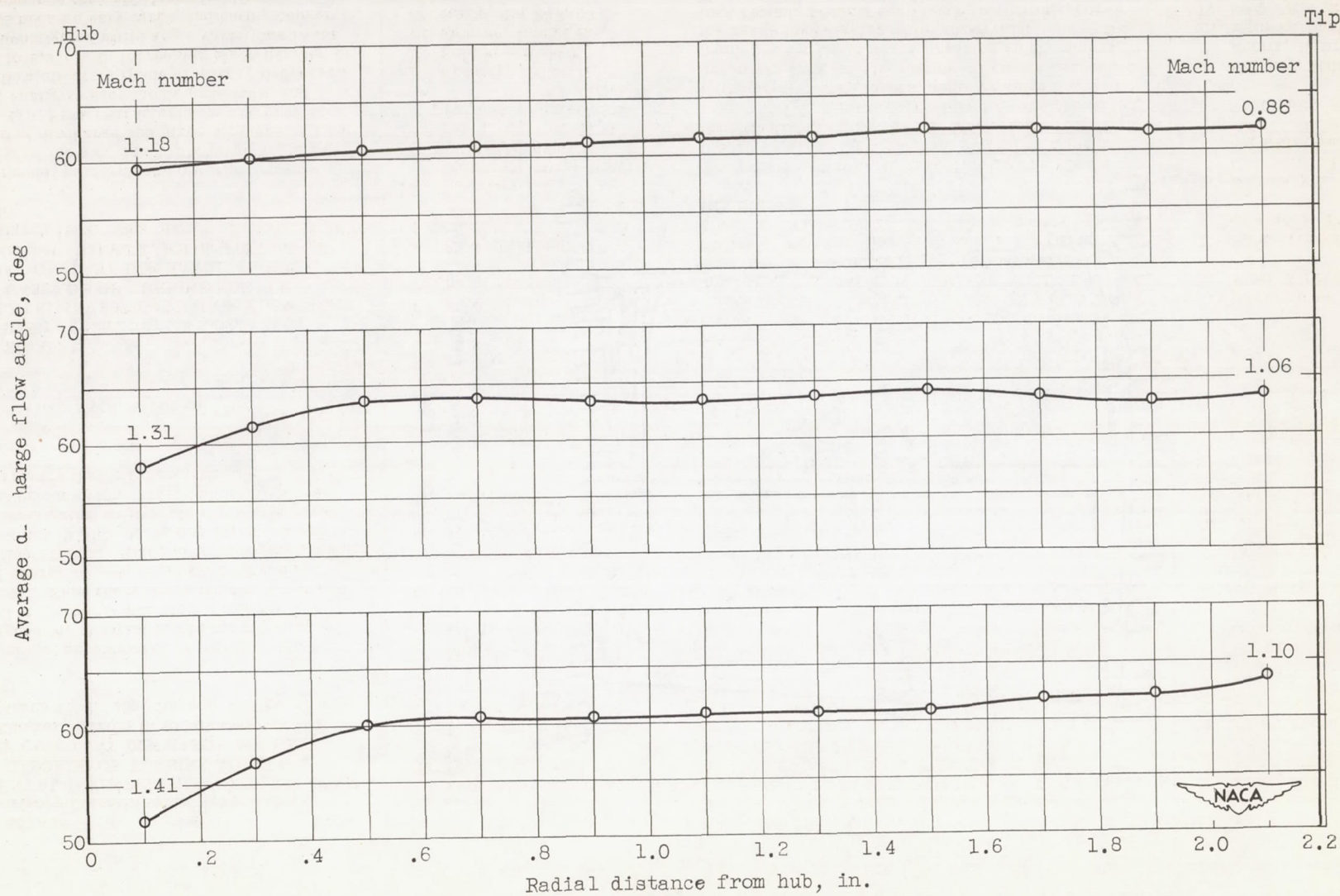


Figure 11. - Average discharge angle.